www.czasopisma.pan.pl PAN www.journals.pan.pl

jet INTL JOURNAL OF ELECTRONICS AND TELECOMMUNICATIONS, YEAR, VOL. 69, NO. 1, PP. 139–146
Manuscript received February 1, 2022; revised February, 2023. DOI: 10.24425/ijet.2023.144343

Improved Two-Dimensional Double Successive Projection Algorithm for Massive MIMO Detection

Sourav Chakraborty, Nirmalendu Bikas Sinha, and Monojit Mitra

***Abstract*—In a massive multiple-input multiple-output (MIMO) system, a large number of receiving antennas at the base station can simultaneously serve multiple users. Linear detectors can achieve optimal performance but require large dimensional matrix inversion, which requires a large number of arithmetic operations. Several low complexity solutions are reported in the literature. In this work, we have presented an improved two-dimensional double successive projection (I2D-DSP) algorithm for massive MIMO detection. Simulation results show that the proposed detector performs better than the conventional 2D-DSP algorithm at a lower complexity. The performance under channel correlation also improves with the I2D-DSP scheme. We further developed a soft information generation algorithm to reduce the number of magnitude comparisons. The proposed soft symbol generation method uses real domain operation and can reduce almost 90% flops and magnitude comparisons.**

***Keywords*—massive MIMO; MMSE; ZF; 2D-DSP; QAM; LLR; I2D-DSP**

I. Introduction

DEMAND for a high data rate in wireless systems motivates the design of efficient techniques. Massive MIMO is one of the key techniques for beyond 5G and future 6G applications [1]. The massive MIMO systems can serve several dozens of users simultaneously using a large number of antennas at the base station [2]. It has been shown in the literature that massive MIMO systems have higher spectral efficiency, energy efficiency and can achieve higher link reliability [3], [4]. However, the complexity of detection is also increasing as the number of users increases [5]. It has been shown in the literature that linear detectors such as minimum mean square error (MMSE) or zero forcing (ZF) method can achieve optimal performance for massive MIMO detection [4]. However, the computation of MMSE/ZF requires exact matrix inversion, which has a complexity order of $O(N_t^3)$. Therefore, for massive MIMO systems, the complexity is significantly high [2]. The low complexity solutions in literature are categorized in two sections: approximate matrix inversion (AMI) and other is solution vector estimation through iteration. In the case of AMI, such as Neumann method [6], [7], Newton-Schultz [8] iteration, etc. the inversion is required per channel update and relatively higher computational complexity. The AMI is essential for channel matrix precoding in downlink data transmission [9], [10]. On the other hand, estimation of MMSE/ZF solution vector through iteration works on per received signal vector. Our works fall in this category of detection. Several low complexity iterative MMSE detection algorithms are reported in literature such as Richardson iteration (RI) [11], Gauss-Seidel (GS) [12], [13], SOR [14], conjugate gradient (CG) [15], [16], Chebyshev (CHEBY) [17], [18], Jacobi iteration (JI) [5], steepest (ST) [19] etc. However, in massive MIMO system, performance of these algorithms are evaluated based on several conditions like rate of convergence, modulation order, number of required iterations, computational complexity etc [5].

For example, Richardson and Jacobi's method have lower complexity per iteration. Still, its convergence rate is also low, and many iterations are required to achieve the exact MMSE result. On the other hand, the Chebyshev method shows a higher convergence rate at the cost of higher complexity. Gauss-Seidel and SOR are examples of a one-dimensional projection method and show good detection performance, and it requires almost three to four iterations to achieve the optimal solution. But computation of GS and SOR are sequential. Therefore existing algorithms trade off between performance and complexity. Recently reported two-dimensional double successive projection (2D-DSP) [20], [21] method shows good detection performance and is also suitable for higher-order modulations.

The performance of iterative algorithms is critically dependent on selecting the initial solution vector. Several algorithms have addressed this issue earlier by using a hybrid method where the first iteration is replaced by the first iteration of any higher convergent method. For example, in [19], a higher convergent Steepest-Jacobi (ST-JA) method is used to improve the performance of the conventional Jacobi method. In [22], the initial solution is replaced by a higher convergent Newton method to improve the detection performance of the conventional Richardson method. In [23] Richardson and Chebyshev methods are combined to achieve better performance with lower complexity. Motivated by this fact, in this work, we have introduced an improved 2D-DSP method where the first iteration is replaced by the steepest-Jacobi method to achieve better performance.

After getting the MMSE estimate of the received signal vector, the bit-wise log-likelihood ratio (LLR) of soft values

S. Chakraborty is with Department of Electronics and Communication Engineering, Cooch Behar Government Engineering College, Coochbehar, India (e-mail: sourav.chakraborty@cgec.org.in).

N. B. Sinha is Principal, Maharaja Nandakumar Mahavidyalaya, Purba Medinipore, India (e-mail: nbsinha.ece@gmail.com).

M. Mitra are with Department of Electronics and Telecommunication Engineering, IIEST Shibpur, Howrah, India (e-mail: monojit$_m$1@$yahoo.co.in$).

is essential for the channel decoder. However, the exact LLR generation method [6] involves matrix inversion and matrix-matrix multiplications. In a massive MIMO system, matrix dimensions are very large, and the exact LLR generation is not a good choice for practical application. A low complexity approximate LLR generation method is shown in [12] by utilizing the channel hardening phenomenon. Still, the complexity of LLR generation is high, and especially in higher-order modulations, it is significantly large. Therefore, in this work, we have proposed a low complexity approximate LLR generation method, which requires less number of real operations in lower-order and higher-order modulations. Our contributions in this work are summarized as follows:

1) We have developed an improved performance 2D-DSP algorithm. The proposed algorithm has lower complexity and better detection performance than the conventional 2D-DSP algorithm.
2) We have proposed a low complexity bit-wise LLR generation scheme for the channel decoder. The proposed method significantly reduces the number of arithmetic operations and the number of comparisons required per-bit LLR generation. Especially in higher-order modulation like the 256-QAM system, it significantly reduces the number of comparisons.

Outline: Section II will describe the system model and background. Section III will present the proposed method. A soft symbol generation scheme is presented in section IV. The simulation results and complexity analysis discussed in section V. Section VI concludes the work.

Notation: We have considered bold face upper case and lower case letters as matrices and vectors respectively. The real and imaginary part of any complex number z denoted by $\Re(z)$ and $\Im(z)$ respectively. The matrix inverse, conjugate transpose and transpose denoted by $(.)^{-1}$, $(.)^H$ and $(.)^T$ respectively. The $(i,j)^{th}$ element in any matrix $\boldsymbol{G}$ represented by g_{ij}. $\langle \boldsymbol{x}, \boldsymbol{y} \rangle$ defines an inner product operation of $\boldsymbol{x}$ and $\boldsymbol{y}$.

II. System Model and Background

A. System model

In this work we consider an uplink transmission where N_t single antenna users served simultaneously by N_r receive antennas at the base station where $N_r >> N_t$. The information bits in each transmitter is mapped to a M-QAM constellation point in the finite alphabet $\tilde{\mathbb{A}}$ with size M. The average transmit power is $\tilde{E}_s$ per symbol. The symbols then transmitted through a fading channel. The received signal vector at the base station can be expressed as

$$\tilde{\boldsymbol{y}} = \tilde{\boldsymbol{H}}\tilde{\boldsymbol{x}} + \tilde{\boldsymbol{n}} \tag{1}$$

Where, $\tilde{\boldsymbol{y}} \in \mathbb{C}^{N_r \times 1}$ denotes the received vector and $\tilde{\boldsymbol{x}} \in \mathbb{C}^{N_t \times 1}$ denotes the transmitted vector. $\tilde{\boldsymbol{n}} \in \mathbb{C}^{N_r \times 1}$ is the additive white Gaussian noise (AWGN) where each of its entries distributed as $\mathcal{N}(0, \tilde{\sigma}^2)$ and $\tilde{\sigma}^2$ is the noise variance. $\tilde{\boldsymbol{H}} \in \mathbb{C}^{N_r \times N_t}$ is the channel matrix. The $(i,j)^{th}$ entry of $\tilde{\boldsymbol{H}}$ denotes as $\tilde{h}_{ij}$ and defined as the complex channel gain between j^{th} transmit antenna and i^{th} receive antenna. The entries of $\tilde{\boldsymbol{H}}$ are assumed to be zero mean and unit variance and perfectly known at the receiver.

The complex received signal model in (1) can be converted into equivalent real equation by real valued decomposition (RVD) method. Thus (1) can be expressed as:

$$\boldsymbol{y} = \boldsymbol{H}\boldsymbol{x} + \boldsymbol{n} \tag{2}$$

Where, $\boldsymbol{y} = [\Re(\tilde{\boldsymbol{y}}) \ \Im(\tilde{\boldsymbol{y}})]^T$, $\boldsymbol{x} = [\Re(\tilde{\boldsymbol{x}}) \ \Im(\tilde{\boldsymbol{x}})]^T$, $\boldsymbol{n} = [\Re(\tilde{\boldsymbol{n}}) \ \Im(\tilde{\boldsymbol{n}})]^T$ and $\boldsymbol{H} \in \mathbb{R}^{2N_r \times 2N_t}$ is the real equivalent channel matrix and can be expressed as:

$$\boldsymbol{H} = \begin{bmatrix} \Re(\tilde{\boldsymbol{H}}) & -\Im(\tilde{\boldsymbol{H}}) \\ \Im(\tilde{\boldsymbol{H}}) & \Re(\tilde{\boldsymbol{H}}) \end{bmatrix} \tag{3}$$

The symbols in $\boldsymbol{x}$ are selected from real equivalent constellation set $\mathbb{A}$. For example, real equivalent constellation set for 64-QAM is $\mathbb{A} = \{-7, -5, -3, -1, 1, 3, 5, 7\}$. Therefore number of elements in $\mathbb{A}$ is $\sqrt{M}$ for M-QAM constellation. The average symbol energy and noise variance for real equivalent model are $E_s = \tilde{E}_s/2$ and $\sigma^2 = \tilde{\sigma}^2/2$ respectively. Number of bits per complex symbol are $Q = \log_2 M$.

B. MMSE detection

As mentioned earlier, MMSE detection can achieve optimal performance in massive MIMO application. The conventional approach of MMSE detection can be expressed as

$$\hat{\boldsymbol{x}} = (\boldsymbol{H}^T\boldsymbol{H} + \sigma^2\boldsymbol{I}_{\boldsymbol{2N_t}})^{-1}\boldsymbol{H}^T\boldsymbol{y} = \boldsymbol{A}^{-1}\boldsymbol{b} \tag{4}$$

Where, $\boldsymbol{b} = \boldsymbol{H}^T\boldsymbol{y}$ is the matched filter output of $\boldsymbol{y}$ and $\boldsymbol{A} = \boldsymbol{H}^T\boldsymbol{H} + \sigma^2\boldsymbol{I}_{\boldsymbol{2N_t}} = \boldsymbol{G} + \sigma^2\boldsymbol{I}_{\boldsymbol{2N_t}}$ is the MMSE filtering matrix. $\boldsymbol{G} = \boldsymbol{H}^T\boldsymbol{H}$ is the Gram matrix and $\hat{\boldsymbol{x}}$ is the MMSE estimated solution vector.

III. Proposed Algorithm

It has been shown in literature that 2D-DSP [21] algorithm is an efficient way of solving linear equations iteratively. In this section, we shall present an improved version of 2D-DSP (I2D-DSP) algorithm which have relatively lower complexity and improved detection performance. For massive MIMO system, matrix $\boldsymbol{A}$ is diagonally dominant and this allows us to estimate the initial approximate solution as $\boldsymbol{x}^{(\boldsymbol{0})} \approx \boldsymbol{D}^{-1}\boldsymbol{b}$, where, $\boldsymbol{D}$ is a diagonal matrix whose diagonal elements are identical to $\boldsymbol{G}$. Now, as we know, in any iterative detection algorithm, initial solution plays critical role in determining the detection performance. Recently reported joint steepest-Jacobi [19] based initialization method shows good performance improvement in conventional Jacobi based iteration. Hence, in this work we have considered the first iteration of proposed algorithm as

$$\boldsymbol{x}^{(\boldsymbol{1})} = \boldsymbol{x}^{(\boldsymbol{0})} + u\boldsymbol{r}^{(\boldsymbol{0})} + \boldsymbol{D}^{-1}(\boldsymbol{r}^{(\boldsymbol{0})} - u\boldsymbol{p}^{(\boldsymbol{0})}) \tag{5}$$

Where, $\boldsymbol{r}^{(\boldsymbol{0})}$ is the residual term and determined as $\boldsymbol{r}^{(\boldsymbol{0})} = \boldsymbol{b} - \boldsymbol{A}\boldsymbol{x}^{(\boldsymbol{0})}$. Also, $\boldsymbol{p}^{(\boldsymbol{0})} = \boldsymbol{A}\boldsymbol{r}^{(\boldsymbol{0})}$ and $u = \frac{\boldsymbol{r}^{(\boldsymbol{0})T}\boldsymbol{r}^{(\boldsymbol{0})}}{\boldsymbol{p}^{(\boldsymbol{0})T}\boldsymbol{p}^{(\boldsymbol{0})}}$. Using (5) as the initial solution, rest of the iterations in proposed algorithm will follow the same steps as conventional 2D-DSP method [21]. Lets consider, $\mathcal{K}$ and $\mathcal{L}$ be the search subspace and constrained subspace [20]. Then by using Petrov-Galerkin condition, we can determine the approximate solution $\boldsymbol{x}^{(\boldsymbol{k})} \in$

$\boldsymbol{x^{(k-1)}} + \mathcal{K}$ such that the residual $\boldsymbol{r^{(k)}} = \boldsymbol{b} - \boldsymbol{Ax^{(k)}} \perp \mathcal{L}$. Gauss-Seidel method is an one dimensional projection method where, $\mathcal{K} = \mathcal{L} = span\{\boldsymbol{e_i}\}$, where, $\boldsymbol{e_i}$ denotes i^{th} column of the identity matrix. In case of 2D-DSP method, we choose $\mathcal{K} = \mathcal{L} = span\{\boldsymbol{e_m}, \boldsymbol{e_n}\}$, i.e. two successive projections are required. With this, the approximate solution vector at k^{th} iteration can be expressed as:

$$\boldsymbol{x_{i+1}^{(k)}} = \boldsymbol{x_i^{(k)}} + \alpha_i^{(k)} \boldsymbol{e_m} + \beta_i^{(k)} \boldsymbol{e_n} \tag{6}$$

The scalars, $\alpha_i^{(k)}$ and $\beta_i^{(k)}$ computed as

$$\alpha_i^{(k)} = (g_{ij} p_j^{(k)} - g_{jj} p_i^{(k)})/\lambda_i \tag{7}$$

$$\beta_i^{(k)} = (g_{ij} p_i^{(k)} - g_{ii} p_j^{(k)})/\lambda_i \tag{8}$$

The components in (7) and (8) can be determined as: $\lambda_i = g_{ii} g_{jj} - g_{ij}^2$, $p_i^{(k)} = \langle \boldsymbol{g_i}, \boldsymbol{x_i^{(k)}} \rangle - b_i$ and $p_j^{(k)} = \langle \boldsymbol{g_j}, \boldsymbol{x_i^{(k)}} \rangle - b_j$. It is mentioned in [21] that m and n are related by $f = m - n$. Where, f is a constant and choice of f is critical in detection. A typical value $f = 3$ can produce good result. When, $m \leq f$, then the value of n can be selected as $n = m - f + 2N_t$.

Algorithm 1 shows the detailed steps for proposed I2D-DSP algorithm. Initialization performed in line 2. After initialization phase is over, first iteration is performed using joint steepest-Jacobi method (line 4-5). In phase 2, conventional 2D-DSP steps are performed for $K - 1$ iterations.

Algorithm 1 Proposed I2D-DSP algorithm

1: **Input:** $\boldsymbol{H}, \boldsymbol{A}, \boldsymbol{G}, \boldsymbol{y}, \sigma^2, K, f$; **Output:** $\hat{\boldsymbol{x}}$
2: **Initialization:** $\boldsymbol{D} = diag(\boldsymbol{G})$
3: **Phase 1:** Steepest based iteration
4: $\boldsymbol{r^{(0)}} = \boldsymbol{b} - \boldsymbol{Ax^{(0)}}$, $\boldsymbol{p^{(0)}} = \boldsymbol{Ar^{(0)}}$, $u = \frac{\boldsymbol{r^{(0)}}^T \boldsymbol{r^{(0)}}}{\boldsymbol{p^{(0)}}^T \boldsymbol{p^{(0)}}}$
5: $\boldsymbol{x^{(1)}} = \boldsymbol{x^{(0)}} + u\boldsymbol{r^{(0)}} + \boldsymbol{D}^{-1}(\boldsymbol{r^{(0)}} - u\boldsymbol{p^{(0)}})$
6: **Phase 2:** 2D-DSP iteration; $\boldsymbol{d_1^{(1)}} = \boldsymbol{x^{(1)}}$
7: **for** $k = 1$ to $K - 1$ **do**
8: **for** $i = 1$ to $2N_t$ **do**
9: $j = i - f$
10: **if** $i \leq f$ **then**
11: $j = i - f + 2N_t$
12: **end if**
13: $\lambda_i = g_{ii}\ g_{jj} - g_{ij}^2$
14: $p_{ki} = \langle \boldsymbol{g_i}, \boldsymbol{d_i^{(k)}} \rangle - b_i$; $p_{kj} = \langle \boldsymbol{g_j}, \boldsymbol{d_j^{(k)}} \rangle - b_j$
15: $\alpha_{ki} = \frac{g_{ij}\ p_{kj} - g_{jj}\ p_{ki}}{\lambda_i}$; $\beta_{ki} = \frac{g_{ij}\ p_{kj} - g_{jj}\ p_{ki}}{\lambda_i}$
16: $\boldsymbol{d_{i+1}^{(k)}} = \boldsymbol{d_i^{(k)}} + \alpha_{ki}\boldsymbol{e_i} + \beta_{ki}\boldsymbol{e_j}$
17: **end for**
18: $\boldsymbol{d_1^{(k+1)}} = \boldsymbol{d_{2N_t+1}^{(k)}}$
19: **end for**
20: $\hat{\boldsymbol{x}} = \boldsymbol{d_{2N_t+1}^{(K)}}$

IV. Proposed Soft Symbol Generation

After estimation of transmitted signal vector using MMSE method, bit-wise soft information is required to generate for channel decoder. However, generation of soft information requires first the computation of equivalent channel gain and noise-plus-interference (NPI) variance. Lets consider $\boldsymbol{E} = \boldsymbol{A}^{-1}\boldsymbol{G}$ and $\boldsymbol{U} = \boldsymbol{A}^{-1}\boldsymbol{G}\boldsymbol{A}^{-1}$. Then the equivalent channel gain at i^{th} level is expressed as $\mu_i = e_{i,i}$ and the NPI variance computed as [6]

$$v_i^2 = \sum_{n=1, n\neq i}^{2N_t} e_{ni}^2 + u_{ii}\sigma^2 \tag{9}$$

The computation of LLR at i^{th} level of b^{th} bit can be expressed as [6]

$$LLR_{i,b} = \gamma_i \left(\min_{a \in \boldsymbol{S_b^1}} \left| \frac{\hat{x}_i}{\mu_i} - a \right|^2 - \min_{a' \in \boldsymbol{S_b^0}} \left| \frac{\hat{x}_i}{\mu_i} - a' \right|^2 \right) \tag{10}$$

Where, $\gamma_i = \frac{\mu_i^2}{v_i^2}$ is signal to interference noise ratio at i^{th} level. $\boldsymbol{S_b^1}$ and $\boldsymbol{S_b^0}$ are the set of symbols whose b^{th} bit is '1' and '0' respectively. However, computation of μ_i and γ_i involves large dimension matrix inversion and matrix-matrix multiplication. Thus, exact LLR generation method is infeasible for massive MIMO detection. Fortunately channel hardening phenomenon can be used to estimate inverse of $\boldsymbol{A}$ as $\boldsymbol{A}^{-1} \approx \boldsymbol{G}^{-1} \approx \boldsymbol{D}^{-1}$. Thus, the matrices required to compute mean and variance are approximated as $\boldsymbol{E} \approx \boldsymbol{D}^{-1}\boldsymbol{G}$ and $\boldsymbol{U} \approx \boldsymbol{D}^{-1}\boldsymbol{G}\boldsymbol{D}^{-1}$ [12]. As $\boldsymbol{D}^{-1}$ is a diagonal matrix, significantly low complexity is required to compute $\boldsymbol{E}$ and $\boldsymbol{U}$. However, even if the diagonal matrix approximation reduces the complexity, computation of (9) for all levels is almost equivalent to multiplication of two $2N_t \times 2N_t$ matrices and have computational complexity $O(N_t^3)$. Using simulation, we noticed that $\sum_{n=1, n\neq i}^{2N_t} e_{ni}^2 << u_{ii}\sigma^2$ in (9) for massive MIMO system. We also observed that, the expected value of $\sum_{n=1, n\neq i}^{2N_t} e_{ni}^2$ is converges towards N_t/N_r. Hence, we can simplify (9) as:

$$v_i^2 \approx \frac{N_t}{N_r} + u_{ii}\sigma^2 \tag{11}$$

This approximation significantly reduces the number of arithmetic operations for LLR computation. After computation of mean and NPI, next step is to determine the LLR values for each bit. As seen from (10), two minimum values required to compute LLR for each bit. In case of complex domain operation, searching complexity is significantly high as searching is performed over $M/2$ terms. For example, in 256-QAM system, 128 comparisons as well as 128 number of $z = \left| \frac{\hat{x}_i}{\mu_i} - a \right|^2$ terms required to compute for each minimum value computation in (10). Therefore, for higher order modulations, conventional complex domain method is not a good choice. In real valued system, the number of comparisons reduces to $\sqrt{M}/2$ which is much lower than complex domain computation. Thus, in proposed method, we shall consider real valued system for bit wise LLR computation. In spite of all these approximations and simplifications, computation of (10) still have redundancy in its operation. Hence, we shall now present an efficient method for LLR generation in this section. Table I and table II shows the real equivalent symbols, corresponding gray coded bit pattern and index for each symbol for 64-QAM and 256-QAM modulations schemes. Same can be done for other modulations also. Based on table I or table II, we can generate two look-up tables $\boldsymbol{I^{(0)}}$ and $\boldsymbol{I^{(1)}}$, containing index values for each modulation scheme. The i^{th} row of $\boldsymbol{I^{(0)}}$ indicated the symbol indices which have i^{th} bit

TABLE I
MAPPING OF SYMBOL BIT AND INDEX FOR REAL EQUIVALENT CONSTELLATION OF 64-QAM

Symbol	Bit pattern	index	Symbol	Bit pattern	index
−7	000	1	7	100	7
−5	001	2	5	101	8
−3	011	4	3	111	6
−1	010	3	1	110	5

TABLE II
MAPPING OF SYMBOL BIT AND INDEX FOR REAL EQUIVALENT CONSTELLATION OF 256-QAM

Symbol	Bit pattern	index	Symbol	Bit pattern	index
−15	0000	1	15	1000	9
−13	0001	2	13	1001	10
−11	0011	4	11	1011	12
−9	0010	3	9	1010	11
−7	0110	7	7	1110	15
−5	0111	8	5	1111	16
−3	0101	6	3	1101	14
−1	0100	5	1	1100	13

'0'. Similarly, i^{th} row of $\boldsymbol{I^{(1)}}$ indicated the symbol indices which have i^{th} bit '1'. For example, in a 64-QAM modulated system, $\boldsymbol{I^{(0)}}$ and $\boldsymbol{I^{(1)}}$ can be represented as:

$$\boldsymbol{I^{(0)}} = \begin{bmatrix} 1 & 2 & 4 & 3 \\ 1 & 2 & 6 & 5 \\ 1 & 3 & 7 & 5 \end{bmatrix}, \boldsymbol{I^{(1)}} = \begin{bmatrix} 7 & 8 & 6 & 5 \\ 4 & 3 & 7 & 8 \\ 2 & 4 & 8 & 6 \end{bmatrix} \quad (12)$$

$\boldsymbol{I^{(0)}}$ and $\boldsymbol{I^{(1)}}$ for other modulation schemes can be constructed in a similar way. Now, if we look at the LLR expression in (10) carefully, we can notice that for each real symbol, one of these minimum value is common to all of its bits. Therefore, at i^{th} level ($i = 1, 2, \ldots, 2N_t$) we shall compute all the possible values of $z = \left|\frac{\hat{x}_i}{\mu_i} - a\right|^2$, where $a \in \mathbb{A}$. Next, minimum value of z is determined and corresponding symbol bit pattern is evaluated. Hence, at i^{th} level, $\sqrt{M}$ terms required to compute. Note that, in conventional method, $\sqrt{M}$ values of z required to evaluate per bit LLR generation. Whereas, proposed method requires $\sqrt{M}$ values of z per $log_2\sqrt{M}$ bits. For each bit LLR generation only one minimum required to determine out of $\sqrt{M}/2$ terms. The algorithm 2 shows the detailed steps for LLR generation. At the preprocessing step, all mean and NPI values are computed. Note that, these values required to update only once per channel update. Next is detection phase where, the MMSE estimation is performed using either exact or any iterative method. Last LLR computation is performed.

V. SIMULATION RESULTS

This section will show the analysis of the proposed algorithm and compare it with existing state-of-art methods. First, we shall examine the uncoded bit error rate (BER) performance. Next, the performance in the coded MIMO system is presented. In all cases, the performance of the exact MMSE detector is considered optimal and referenced to other methods. Last, the complexity analysis is presented.

Algorithm 2 Proposed low complexity LLR generation

Input: $\boldsymbol{A}, \hat{\boldsymbol{x}}$; **Output:** $\boldsymbol{LLR}$
Initialization: $\boldsymbol{D} = diag(\boldsymbol{A})$; $\boldsymbol{E} = \boldsymbol{D}^{-1}\boldsymbol{G}$; $\boldsymbol{U} = \boldsymbol{E}\boldsymbol{D}^{-1}$
for $i = 1$ to $2N_t$ **do**
  $\mu_i = e_{ii}$; $v_i^2 = \frac{N_r}{N_t} + \sigma^2 u_{ii}$; $\gamma_i = \frac{\mu_i^2}{v_i^2}$
  $z_j = |\frac{x_i}{\mu_i} - a|$, Where, $j = 1, 2, \ldots \sqrt{M}$ and $a \in \mathbb{A}$
  Find the minimum value of $\boldsymbol{z}$, denoted by z_{min} and corresponding index i_{zmin}.
  Obtain bit pattern $\boldsymbol{d}$ corresponding to index i_{zmin} using either table I or II
  for $b = 1$ to $Q/2$ **do**
    if $d_i == 1$ **then**
      $L_1 = z_{min}$
      $L_0 = \underset{i \in \boldsymbol{I_b^{(1)}}}{min}\ z_i$
    else
      $L_0 = z_{min}$
      $L_1 = \underset{i \in \boldsymbol{I_b^{(0)}}}{min}\ z_i$
    end if
  end for
  $LLR_j = \gamma_i(L_0 - L_1)$; $j = j + 1$
end for

A. Uncoded MIMO performance

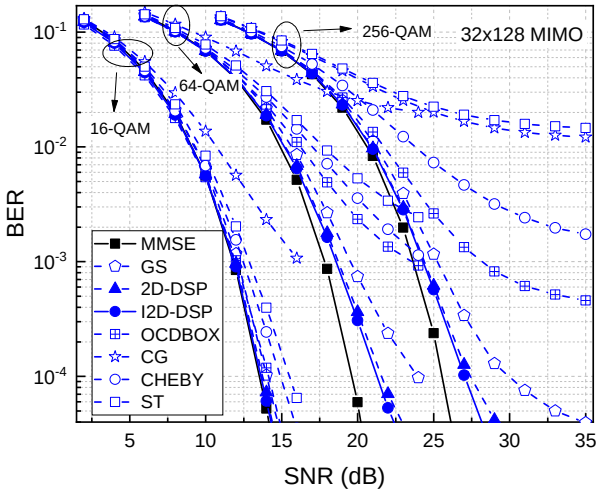

Fig. 1. BER performance of 32 × 128 MIMO system with 16-QAM, 64-QAM and 256-QAM modulation with perfect channel state information

Fig. 1 shows the uncoded BER performance for different modulation scheme where, $K = 3$ for 16-QAM and 64-QAM, and $K = 4$ for 256-QAM. In the case of the 16-QAM modulated system, all the methods except CG perform close to the exact MMSE detector. In the case of the 64-QAM system, GS, 2D-DSP, I2D-DSP achieve close to optimal performance. We notice that I2D-DSP performs slightly better than 2D-DSP in 64-QAM modulated system. Considerable performance degradation can be noticed for CG, CHEBY, OCDBOX and ST-JA in 256-QAM modulated systems. However, in this case, also proposed detector outperforms other algorithms.
The effect of the number of iteration K on BER performance is presented in Fig. 2. We can observe that the proposed I2D-DSP

method can achieve near exact MMSE performance with only two iterations for 16-QAM modulation. As the modulation order increases, more iterations are required to achieve exact MMSE performance. In all the cases, the proposed I2D-DSP performs slightly better than the 2D-DSP method. In the 256-QAM modulated system, GS and OCDBOX require almost five iterations to achieve optimal performance, whereas CG, CHEBY and ST-JA failed to converge near-optimal solutions.

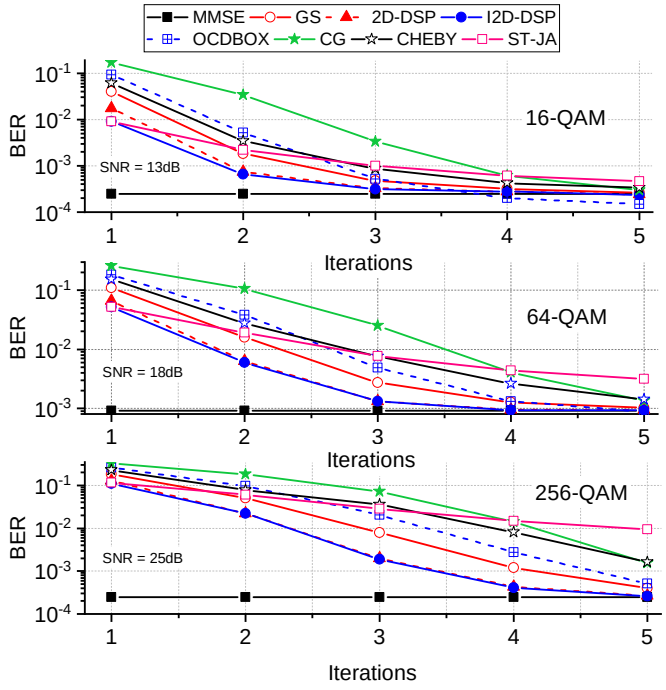

Fig. 2. Effect of algorithm iteration on bit error rate performance for 16×64 MIMO system with 16-QAM, 64-QAM and 256-QAM modulation

Fig. 3 shows the BER variation with the receive antennas keeping $N_t = 16$ and $SNR = 13dB$. The modulation scheme is 64-QAM, and the number of iterations is set to $K = 3$. We can see 2D-DSP and proposed I2D-DSP performance matches to exact MMSE performance when $N_r \geq 4N_t$. For other algorithms, a performance gap with exact can be noticeable. Further, the performance of all the algorithms improves as N_r increases. Next, we have considered the effect of spatial correlation on BER performance as it plays a critical role in massive MIMO systems. We have considered the Kronecker model for correlated channel matrix, which can be defined as [24]:

$$\boldsymbol{H_c} = \boldsymbol{\phi_r^{1/2}} \boldsymbol{H_{iid}} \boldsymbol{\phi_t^{1/2}} \tag{13}$$

Where, $\boldsymbol{\phi_r^{1/2}} \in \mathbb{C}^{N_r \times N_r}$ and $\boldsymbol{\phi_t^{1/2}} \in \mathbb{C}^{N_t \times N_t}$ are the receive and transmit correlation matrices respectively. A well known exponential model [25] is adapted for correlated matrices. In this work we have considered $\boldsymbol{H_{iid}} = \tilde{\boldsymbol{H}}$. After determining $\boldsymbol{H_c}$, we convert the complex model to real equivalent model through RVD as defined in (3).

The entries of $\boldsymbol{\phi_r}$ and $\boldsymbol{\phi_t}$ determined by correlation factor ζ $(0 \leq \zeta \leq 1)$. Where, $\zeta = 0$ defines no correlation and $\zeta = 1$ is fully correlated channel scenario. For single-antenna users, transmit correlation matrix can be replaced by an identity matrix. Fig. 4 shows the SNR versus BER performance of MMSE, GS, 2D-DSP, and I2D-DSP algorithms for different correlation factors. At the higher correlated channel, where $\zeta = 0.7$, we notice algorithms diverge more from the optimal solution. Overall proposed I2D-DSP shows more robustness in correlated channels than other iterative methods. The significance of correlation magnitude variation on BER performance at a certain SNR is shown in Fig. 5. The SNR is set to $14dB$ and $18dB$ for 16-QAM and 64-QAM modulate systems. At lower correlation, GS, 2D-DSP, and I2D-DSP maintain optimal performance with 64-QAM modulation.

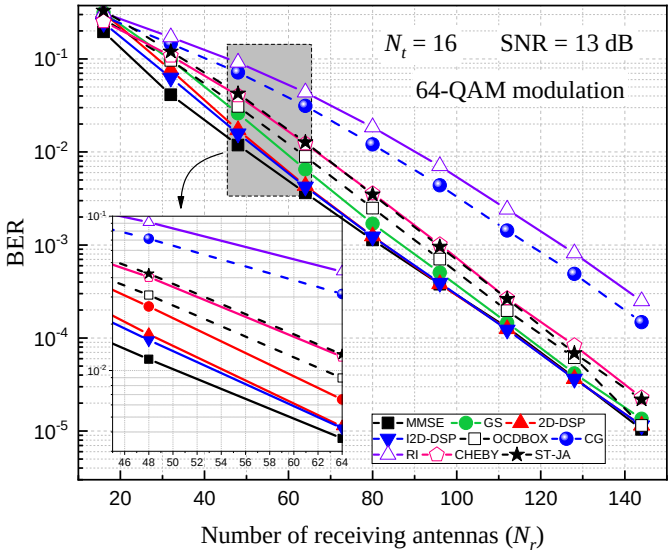

Fig. 3. Effect of receive antenna variation on BER performance

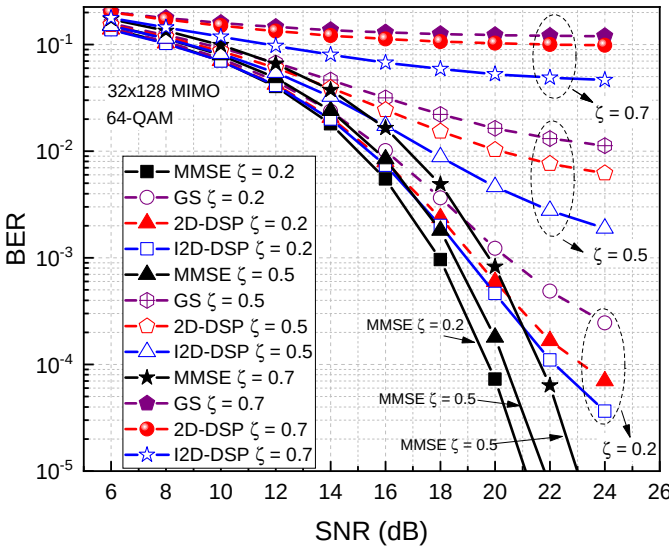

Fig. 4. Effect of correlation on BER performance for 32×128 MIMO system with 64-QAM modulation

However, significant performance loss can be observed at a higher correlation for all methods. Also, compared to 16-QAM, performance loss in 64-QAM is more. I2D-DSP shows better immunity than 2D-DSP against correlation magnitude variation in both cases.

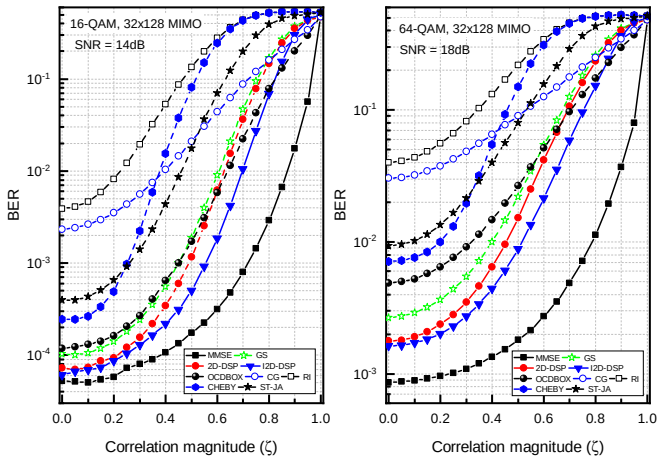

Fig. 5. Effect of correlation magnitude variation on bit error rate performance for 32×128 MIMO system with 16-QAM and 64-QAM modulation

B. Coded MIMO performance

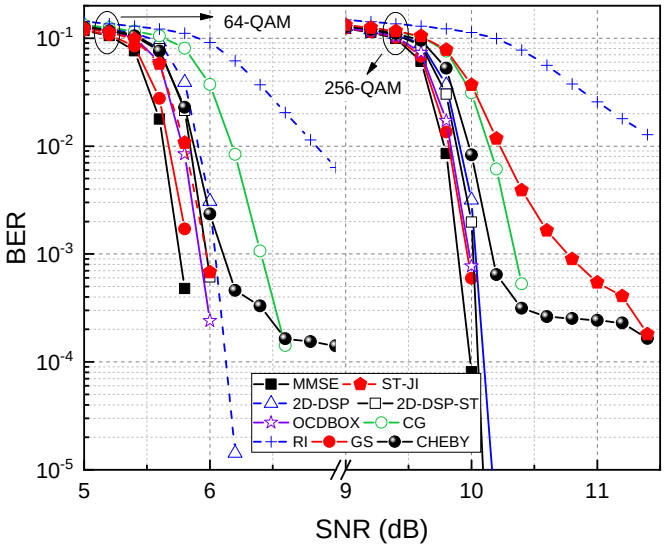

Fig. 6. BER performance of LDPC coded, 32×128 MIMO system with 64-QAM and 256-QAM modulation

Fig. 6 shows the BER performance of 32×128 MIMO system with 64-QAM and 256-QAM modulation for different algorithms. An LDPC code with code length 64800 and code rate $1/2$ is utilized for simulation purposes. The number of iterations for all detectors is set to $K = 3$. For LLR generation, we have considered algorithm 2. The resulting plot shows that all the methods except CG can achieve optimal performance. However, in the 256-QAM system, the performance of CHEBY, CG, ST-JA significantly degrades. In this case, I2D-DSP, 2D-DSP, and GS also show optimal performance. In all cases, the proposed I2D-DSP performs relatively better than 2D-DSP. Fig. 7 compares the performance of different LLR generation methods in 32×128 MIMO system with 64-QAM modulation scheme.We can notice that the proposed LLR generation method and the approx1 LLR generation [12] performs almost identically. However, the performance of approx2 LLR [26] is relatively poor compared to the proposed method.

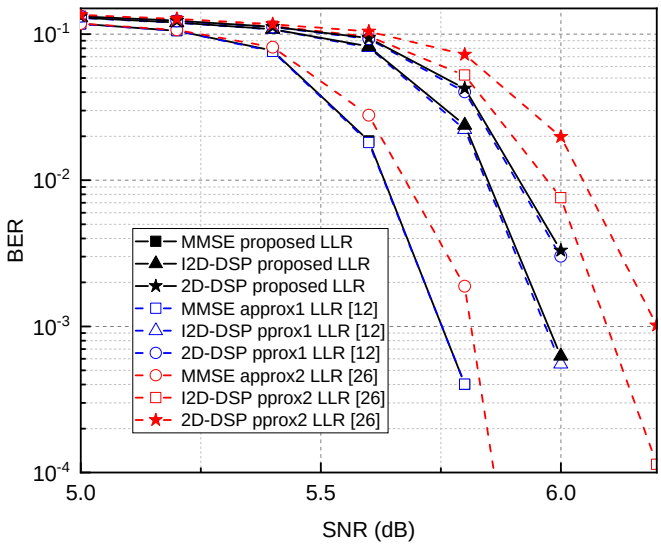

Fig. 7. BER performance comparison between different LLR generation methods

C. Complexity analysis

This section will compare the complexity of the proposed detection and LLR generation with the existing method. All the comparisons are performed in the real domain. We have considered each real arithmetic operation like addition, subtraction, multiplication and division as a flop. Therefore each complex addition and multiplication is equivalent to two and six flops, respectively. For all methods, we have assumed that Gram matrix $\boldsymbol{G} = \boldsymbol{H}^T\boldsymbol{H}$ is available, and hence its complexity is not included in our complexity comparisons.

In proposed algorithm 1, first matched filter output is computed which requires $8N_tN_r - 2N_t$ flops. Computing initial residue term $\boldsymbol{r}^{(0)} = \boldsymbol{b} - \boldsymbol{A}\boldsymbol{x}^{(0)}$ requires $8N_t^2$ flops. The number of flops required in phase 1 of algorithm 1 are $16N_t^2 + 18N_t$. In phase 2 of algorithm 1, $(K-1)$ iterations are performed using conventional 2D-DSP method and it requires total $2(K-1)N_t(8N_t+15)$ flops. In table V we summarized total flops required by different algorithms. From table V we notice that proposed I2D-DSP requires slightly less number of flops than conventional 2D-DSP method. Fig. 8 shows the number of required flops with transmit antenna variation for different detection methods.

Next, we shall discuss the LLR generation complexity with existing methods. The number of operations required for LLR generation can be separated into two parts. First is the computation of approximate mean and variance. The second is bit-wise LLR computation. We notice from algorithm 2 that μ_i and γ_i do not depend on the received signal vector and are only dependent on the channel matrix. Hence, μ_i and γ_i need to be updated only once per channel update, and it is a part of preprocessing. Thus, total $2N_t$ flops are required for all μ_i computations. Similarly, the variance terms determined using $\boldsymbol{U} \approx \boldsymbol{D}^{-1}\boldsymbol{G}\boldsymbol{D}^{-1} \approx \boldsymbol{E}\boldsymbol{D}^{-1}$ and requires additional $2N_t$ multiplications. Further, computation of (11) need $4N_t$ flops. Therefore, total $8N_t$ flops are required in the precomputation phase of the proposed algorithm, which is significantly lower than other computations.

TABLE III
NUMBER OF FLOPS AND COMPARISONS REQUIRED FOR LLR PREPROCESSING AND BIT-WISE LLR COMPUTATION

Method	LLR preprocessing flops	LLR flops	Comparisons
Proposed	$8N_t$	$6N_t\sqrt{M}+4N_t$	$\frac{N_t}{2}(4\sqrt{M}+Q\sqrt{M}-1)$
approximate1 [12]	$4N_t^2(N_t-2)$	$N_t(11QM+2)$	N_tQM
approximate2 [26]	N_t	$N_t(11QM+2)$	N_tQM

TABLE IV
NUMBER OF FLOPS AND REAL VALUE COMPARISONS REQUIRED FOR 32×128 MIMO SYSTEM LLR GENERATION

Method	LLR preprocessing flops	16-QAM		64-QAM		256-QAM	
		LLR flops	Comparisons	LLR flops	Comparisons	LLR flops	Comparisons
Proposed	256	896	496	1.664×10^3	1.264×10^3	3.2×10^3	3.056×10^3
approximate1 [12]	1.228×10^5	2.259×10^4	2048	1.352×10^5	1.228×10^4	7.209×10^5	6.553×10^4
approximate2 [26]	32	2.259×10^4	2048	1.352×10^5	1.228×10^4	7.209×10^5	6.553×10^4

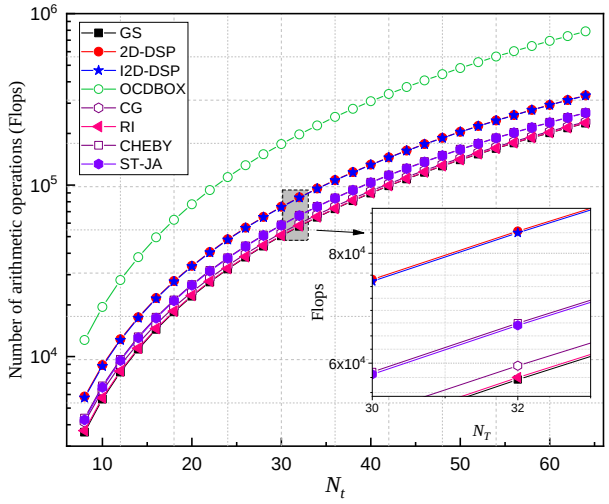

Fig. 8. Number of flops required with transmit antenna variation

In bit-wise LLR computation phase, only arithmetic computation required to evaluate the term $\left|\frac{\hat{x}_i}{\mu_i}-a\right|^2$ for $\sqrt{M}$ real symbols. Therefore, total $3\sqrt{M}$ flops are required at i^{th} level of algorithm 1. The total flops required for whole received vector LLR generation are $6N_t\sqrt{M}+4N_t$. Apart from the arithmetic operations, LLR computation involves a large number of magnitude comparisons to determine the minimum values as indicated in (10). In the proposed method of LLR generation, we first find one minimum per level (line 11 and 14, algorithm 2), which requires $\sqrt{M}-1$ comparisons. Next, for each bit, only one minimum is needed, and in this case, only $\sqrt{M}/2$ number of comparisons are required. Therefore total comparisons required by the proposed LLR generation are

$$N_{comp}=N_t(4\sqrt{M}+Q\sqrt{M}-1)/2 \tag{14}$$

Table III shows the number of arithmetic computations (flops) and comparisons required for different LLR generation methods. It can be noticed that proposed and approximate2 [26] requires an almost negligible number of flops at preprocessing stage. In case of bit-wise LLR generation phase, arithmetic complexity of proposed method is $O(N_t\sqrt{M})$. Whereas other two methods in table III have arithmetic complexity $O(N_tQM)$. The number of comparisons required for N_tQ bits (i.e. the number of bits per transmitted symbol vector) LLR generation is significantly less in the proposed method. The searching complexity of the proposed method is the order of $O(N_tQ\sqrt{M})$ whereas in the conventional method, it is $O(N_tQM)$. Table IV shows the number of operations required for LLR generation in a 32×128 MIMO system with 16-QAM, 64-QAM and 256-QAM modulations. In all cases, proposed LLR generation can reduce more than 90% arithmetic operations and comparisons.

Table VI shows the number of flops required in different detection methods for 32×128 MIMO system with three iterations. Also, we have shown the required SNR to achieve

TABLE V
NUMBER OF FLOPS REQUIRED FOR DIFFERENT DETECTION METHODS.

Method	Number of flops
GS [12]	$8N_tN_r+4N_t+8KN_t^2$
CG [16]	$8N_tN_r-2N_t+8KN_t(N_t+3)$
ST-JA [19]	$8N_tN_r+8N_t^2+16N_t+2KN_t(4N_t+1)$
Chebyshev [18]	$8N_tN_r+8N_t^2+4N_t+2KN_t(4N_t+5)$
OCDBOX [27]	$8KN_t(2N_r+1)$
2D-DSP [21]	$8N_tN_r+2KN_t(8N_t+15)$
I2D-DSP (prop.)	$8N_tN_r-12N_t+2KN_t(8N_t+15)$

TABLE VI
NUMBER OF FLOPS AND SNR REQUIRED TO ACHIEVE A BER OF 10^{-3} FOR 32×128 MIMO SYSTEM

Method	Number of flops ($\times10^4$)	16-QAM SNR (dB)	64-QAM SNR (dB)
GS [12]	5.747	12.3177	19.7304
CG [16]	5.958	16.1408	–
ST-JA [19]	6.624	13.2567	–
Chebyshev [18]	6.662	12.8407	25.0030
OCDBOX [27]	19.737	12.0518	23.6379
2D-DSP [21]	8.480	11.9825	19.0982
I2D-DSP (prop.)	8.441	11.9582	18.9495

a BER of 10^{-3} for different algorithms. CG and ST-JA failed to converge for 64-QAM modulation. We notice that number of required flops in I2D-DSP is slightly lower than 2D-DSP. Performance-wise, I2D-DSP also requires lower SNR than other methods in the case of both 16-QAM and 64-QAM modulation. The proposed I2D-DSP required $0.024dB$ and $0.1487dB$ less SNR than 2D-DSP in 16-QAM and 64-QAM modulations.

VI. Conclusions

In this work, we have proposed an improved performance I2D-DSP algorithm. The complexity analysis shows that the proposed method requires fewer arithmetic operations than the conventional 2D-DSP method. Performance analysis shows that the proposed method outperforms 2D-DSP and other existing algorithms in uncoded systems. Furthermore, the proposed I2D-DSP shows better immunity against correlation magnitude variation under spatially correlated channel scenarios. Further, a low complexity LLR generation method is developed in this work. The proposed LLR generation method reduces almost 90% of flops and numerical comparisons. Also, detection performance in a coded MIMO system using the proposed LLR generation method is close to the conventional method.

References

[1] N. Shlezinger, G. C. Alexandropoulos, M. F. Imani, Y. C. Eldar, and D. R. Smith, "Dynamic Metasurface Antennas for 6G Extreme Massive MIMO Communications," *IEEE Wireless Communications*, vol. 28, no. 2, pp. 106–113, 2021. https://doi.org/10.1109/MWC.001.2000267

[2] F. Rusek, D. Persson, B. K. Lau, E. G. Larsson, T. L. Marzetta, O. Edfors, and F. Tufvesson, "Scaling up mimo: Opportunities and challenges with very large arrays," *IEEE Signal Processing Magazine*, vol. 30, no. 1, pp. 40–60, 2013. https://doi.org/10.1109/MSP.2011.2178495

[3] H. Q. Ngo, E. G. Larsson, and T. L. Marzetta, "Energy and spectral efficiency of very large multiuser mimo systems," *IEEE Transactions on Communications*, vol. 61, no. 4, pp. 1436–1449, 2013. https://doi.org/10.1109/TCOMM.2013.020413.110848

[4] E. G. Larsson, O. Edfors, F. Tufvesson, and T. L. Marzetta, "Massive mimo for next generation wireless systems," *IEEE Communications Magazine*, vol. 52, no. 2, pp. 186–195, 2014. https://doi.org/10.1109/MCOM.2014.6736761

[5] M. A. Albreem, M. Juntti, and S. Shahabuddin, "Massive mimo detection techniques: A survey," *IEEE Communications Surveys Tutorials*, vol. 21, no. 4, pp. 3109–3132, 2019. https://doi.org/10.1109/COMST.2019.2935810

[6] M. Wu, B. Yin, G. Wang, C. Dick, J. R. Cavallaro, and C. Studer, "Large-scale mimo detection for 3gpp lte: Algorithms and fpga implementations," *IEEE Journal of Selected Topics in Signal Processing*, vol. 8, no. 5, pp. 916–929, 2014. https://doi.org/10.1109/JSTSP.2014.2313021

[7] D. Zhu, B. Li, and P. Liang, "On the matrix inversion approximation based on neumann series in massive mimo systems," in *IEEE International Conference on Communications (ICC)*, 2015, pp. 1763–1769. https://doi.org/10.1109/ICC.2015.7248580

[8] J. Minango and C. de Almeida, "Low complexity zero forcing detector based on newton-schultz iterative algorithm for massive mimo systems," *IEEE Transactions on Vehicular Technology*, vol. 67, no. 12, pp. 11 759–11 766, 2018. https://doi.org/10.1109/TVT.2018.2874811

[9] C. Zhang, Z. Li, L. Shen, F. Yan, M. Wu, and X. Wang, "A low-complexity massive mimo precoding algorithm based on chebyshev iteration," *IEEE Access*, vol. 5, pp. 22 545–22 551, 2017. https://doi.org/10.1109/ACCESS.2017.2760881

[10] T. Xie, Q. Han, H. Xu, Z. Qi, and W. Shen, "A low-complexity linear precoding scheme based on sor method for massive mimo systems," in *IEEE 81st Vehicular Technology Conference (VTC Spring)*, 2015, pp. 1–5. https://doi.org/10.1109/VTCSpring.2015.7145618

[11] B. Kang, J.-H. Yoon, and J. Park, "Low-complexity massive mimo detectors based on richardson method," *ETRI Journal*, vol. 39, no. 3, pp. 326–335, 2017. https://doi.org/10.4218/etrij.17.0116.0732

[12] L. Dai, X. Gao, X. Su, S. Han, C.-L. I, and Z. Wang, "Low-complexity soft-output signal detection based on gauss–seidel method for uplink multiuser large-scale mimo systems," *IEEE Transactions on Vehicular Technology*, vol. 64, no. 10, pp. 4839–4845, 2015. https://doi.org/10.1109/TVT.2014.2370106

[13] Z. Wu, C. Zhang, Y. Xue, S. Xu, and X. You, "Efficient architecture for soft-output massive mimo detection with gauss-seidel method," in *IEEE International Symposium on Circuits and Systems (ISCAS)*, 2016, pp. 1886–1889. https://doi.org/10.1109/ISCAS.2016.7538940

[14] X. Gao, L. Dai, Y. Hu, Z. Wang, and Z. Wang, "Matrix inversion-less signal detection using sor method for uplink large-scale mimo systems," in *IEEE Global Communications Conference*, Dec 2014, pp. 3291–3295. https://doi.org/10.1109/GLOCOM.2014.7037314

[15] B. Yin, M. Wu, J. R. Cavallaro, and C. Studer, "Conjugate gradient-based soft-output detection and precoding in massive mimo systems," in *IEEE Global Communications Conference*, Dec 2014, pp. 3696–3701. https://doi.org/10.1109/GLOCOM.2014.7037382

[16] M. Wu, C. Dick, J. R. Cavallaro, and C. Studer, "Fpga design of a coordinate descent data detector for large-scale mu-mimo," in *IEEE International Symposium on Circuits and Systems (ISCAS)*, 2016, pp. 1894–1897. https://doi.org/10.1109/ISCAS.2016.7538942

[17] X. Liu and J. Zhang, "A signal detection algorithm based on chebyshev accelerated symmetrical successive over-relaxation iteration for massive mimo system," in *9th International Conference on Wireless Communications and Signal Processing (WCSP)*, Oct 2017, pp. 1–6. https://doi.org/10.1109/WCSP.2017.8171111

[18] G. Peng, L. Liu, P. Zhang, S. Yin, and S. Wei, "Low-computing-load, high-parallelism detection method based on chebyshev iteration for massive mimo systems with vlsi architecture," *IEEE Transactions on Signal Processing*, vol. 65, no. 14, pp. 3775–3788, July 2017. https://doi.org/10.1109/TSP.2017.2698410

[19] X. Qin, Z. Yan, and G. He, "A near-optimal detection scheme based on joint steepest descent and jacobi method for uplink massive mimo systems," *IEEE Communications Letters*, vol. 20, no. 2, pp. 276–279, Feb 2016. https://doi.org/10.1109/LCOMM.2015.2504506

[20] Y.-F. Jing and T.-Z. Huang, "On a new iterative method for solving linear systems and comparison results," *Journal of Computational and Applied Mathematics*, vol. 220, no. 1, pp. 74–84, 2008. https://doi.org/10.1016/j.cam.2007.07.035

[21] X. Jing, J. Wen, and H. Liu, "Low-complexity soft-output signal detector for massive mimo with higher order qam constellations," *Digital Signal Processing*, vol. 108, p. 102886, 2021. https://doi.org/10.1016/j.dsp.2020.102886

[22] F. Jin, Q. Liu, H. Liu, and P. Wu, "A low complexity signal detection scheme based on improved newton iteration for massive mimo systems," *IEEE Communications Letters*, vol. 23, no. 4, pp. 748–751, April 2019. https://doi.org/10.1109/LCOMM.2019.2897798

[23] I. A. Khoso, X. Dai, M. N. Irshad, A. Khan, and X. Wang, "A low-complexity data detection algorithm for massive mimo systems," *IEEE Access*, vol. 7, pp. 39 341–39 351, 2019. https://doi.org/10.1109/ACCESS.2019.2907366

[24] J. Kermoal, L. Schumacher, K. Pedersen, P. Mogensen, and F. Frederiksen, "A stochastic mimo radio channel model with experimental validation," *IEEE Journal on Selected Areas in Communications*, vol. 20, no. 6, pp. 1211–1226, 2002. https://doi.org/10.1109/JSAC.2002.801223

[25] B. E. Godana and T. Ekman, "Parametrization based limited feedback design for correlated mimo channels using new statistical models," *IEEE Transactions on Wireless Communications*, vol. 12, no. 10, pp. 5172–5184, 2013. https://doi.org/10.1109/TWC.2013.092013.130045

[26] L. Liu, G. Peng, P. Wang, S. Zhou, Q. Wei, S. Yin, and S. Wei, "Energy- and area-efficient recursive-conjugate-gradient-based mmse detector for massive mimo systems," *IEEE Transactions on Signal Processing*, vol. 68, pp. 573–588, 2020. https://doi.org/10.1109/TSP.2020.2964234

[27] M. Wu, C. Dick, J. R. Cavallaro, and C. Studer, "High-throughput data detection for massive mu-mimo-ofdm using coordinate descent," *IEEE Transactions on Circuits and Systems I: Regular Papers*, vol. 63, no. 12, pp. 2357–2367, 2016. https://doi.org/10.1109/TCSI.2016.2611645